

# MicroRNA-21 Knockdown Disrupts Glioma Growth *In vivo* and Displays Synergistic Cytotoxicity with Neural Precursor Cell-Delivered S-TRAIL in Human Gliomas

Maarten F. Corsten,<sup>1</sup> Rafael Miranda,<sup>1</sup> Randa Kasmieh,<sup>1</sup> Anna M. Krichevsky,<sup>2</sup> Ralph Weissleder,<sup>1</sup> and Khalid Shah<sup>1</sup>

<sup>1</sup>Center for Molecular Imaging, Massachusetts General Hospital, and <sup>2</sup>Department of Neurology, Brigham and Women's Hospital, Harvard Medical School, Boston, Massachusetts

## Abstract

Despite the development of new glioma therapies that allow for tumor-targeted *in situ* delivery of cytotoxic drugs, tumor resistance to apoptosis remains a key impediment to effective treatment. Mounting evidence indicates that microRNAs (miRNA) might play a fundamental role in tumorigenesis, controlling cell proliferation and apoptosis. In gliomas, microRNA-21 (miR-21) levels have been reported to be elevated and their knockdown is associated with increased apoptotic activity. We hypothesized that suppression of miR-21 might sensitize gliomas for cytotoxic tumor therapy. With the use of locked nucleic acid (LNA)-antimiR-21 oligonucleotides, bimodal imaging vectors, and neural precursor cells (NPC) expressing a secretable variant of the cytotoxic agent tumor necrosis factor-related apoptosis inducing ligand (S-TRAIL), we show that the combined suppression of miR-21 and NPC-S-TRAIL leads to a synergistic increase in caspase activity and significantly decreased cell viability in human glioma cells *in vitro*. This phenomenon persists *in vivo*, as we observed complete eradication of LNA-antimiR-21-treated gliomas subjected to the presence of NPC-S-TRAIL in the murine brain. Our results reveal the efficacy of miR-21 antagonism in murine glioma models and implicate miR-21 as a target for therapeutic intervention. Furthermore, our findings provide the basis for developing combination therapies using miRNA modulation and cytotoxic tumor therapies. [Cancer Res 2007;67(19):8994–9000]

## Introduction

Despite the recent advances in therapeutic strategies, such as surgical resection and adjuvant radiotherapy and chemotherapy, the prognosis for patients with brain tumors remains poor. New therapies that provide highly specific tumor cell killing and complete eradication of cancer cells are urgently needed. MicroRNAs (miRNA) are small (~20–22 nucleotides) noncoding RNAs that bind to partially complementary recognition sequences of mRNA, causing either degradation or inhibition of translation, thus effectively silencing their mRNA target (1). This pretranslational level of governance is estimated to affect up to one third of all

human transcripts, including those involved in cancer (1). The tight connection between miRNAs and tumorigenesis is emphasized by the localization of more than 50% of miRNAs near cancer-associated genomic break points, the differential expression profiles of miRNAs from healthy tissue across cancers, and the surprising strength of these profiles in tumor classification and prediction of therapy response (2–6). These findings create a firm rationale for the incorporation of miRNA-targeted treatment strategies in cancer medicine.

Recently, microRNA-21 (miR-21) was shown to be strongly overexpressed in glioblastomas with *in vitro* knockdown of miR-21, using modified antisense oligonucleotides, leading to a significant reduction in cell viability accompanied by elevated intracellular levels of caspases (7). Although the mechanism that underlies these effects is largely unknown, it is tempting to hypothesize that miR-21 somehow favors tumor growth by impeding apoptosis. Such a role would imply attractive opportunities for miR-21 targeting in tumor treatment, as “immunity” to apoptosis represents one of the classic hallmarks of cancers and, as such, is a key factor in resistance to therapy (8, 9). Our first goal in the present study was to confirm feasibility of the previous data *in vivo* by monitoring glioma growth after knockdown of miR-21 in the murine brain while visualizing tumor burden through bioluminescence imaging.

As mentioned, the proapoptotic effect of miR-21 knockdown provides incentive for combination with therapies that exhibit insufficient apoptosis-inducing effect. A capricious growth pattern and the blood-brain barrier form obstacles to conventional glioblastoma treatment, mandating therapeutic alternatives that provide specific homing and local drug delivery (10, 11). One promising approach to local delivery is transgenic “charging” of pathotropic neural precursor cells (NPC) with genes encoding proapoptotic proteins, such as the tumor necrosis factor-related apoptosis inducing ligand (TRAIL). TRAIL selectively induces apoptosis in tumor tissue through binding to death domain-linked receptors while sparing most normal cells (12, 13). However, because its use is complicated by the blood-brain barrier and it has short biological half-life, most studies using TRAIL in gliomas (14, 15) offer promise but lack applicability. To overcome these obstacles, we have previously engineered a secretable form of recombinant TRAIL (S-TRAIL) with enhanced cytotoxic efficacy for glioma cells (16) and then stably transfected NPC to create progenitor cells capable of migrating throughout diseased brain toward tumor main burden and secreting S-TRAIL *in loco* (17).

In this study, we sought to evaluate the combined effect of miR-21 antagonism and NPC-mediated S-TRAIL delivery on glioma growth, *in vitro* as well as *in vivo*, using optical imaging

**Note:** Supplementary data for this article are available at Cancer Research Online (<http://cancerres.aacrjournals.org/>).

**Requests for reprints:** Khalid Shah, Massachusetts General Hospital, Harvard Medical School, Charlestown, MA 02129. Phone: 617-726-4821; Fax: 617-726-5708; E-mail: kshah@helix.mgh.harvard.edu.

©2007 American Association for Cancer Research.  
doi:10.1158/0008-5472.CAN-07-1045

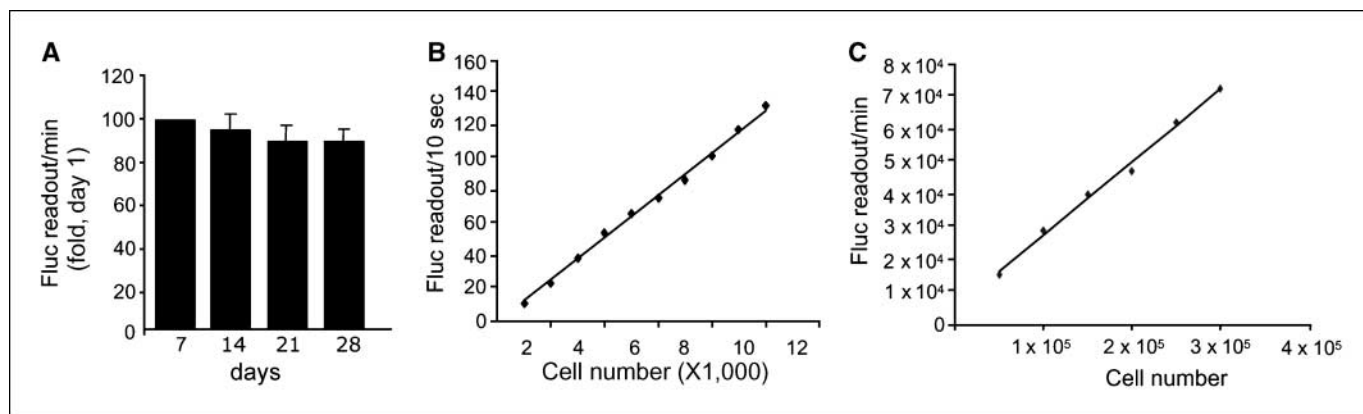


**Figure 1.** Lentiviral mediated stable transgene expression and direct correlation between cell number and bioluminescence intensity. *A*, duration of Fluc-DsRed2 lentiviral transgene expression over time in LV-Fluc-DsRed2-transduced Gli36 glioma cells. *B* and *C*, correlation between Fluc-DsRed2-expressing U87 glioma cells and bioluminescent signal intensity in culture (*B*) and *in vivo* (*C*).

to simultaneously monitor glioma proliferation and NPC survival. We report here that combining miR-21 knockdown with S-TRAIL leads to synergistic cytotoxicity, which is associated with enhanced caspase activity *in vitro*, and results in significant reduction of tumor growth *in vivo* as compared with either monotherapy.

## Materials and Methods

### Generation of lentiviruses encoding S-TRAIL and optical markers.

The lentiviral transfer plasmids used to generate the lentiviruses utilized in this study have previously been described (18). Three lentiviral vectors were used: (a) LV-Fluc-DsRed2 bearing a cDNA fusion of firefly luciferase and DsRed2 under the cytomegalovirus (CMV) promoter;<sup>3</sup> (b) LV-S-TRAIL bearing S-TRAIL cDNA (16) in front of the CMV promoter and also containing an IRES-GFP cassette (18); and (c) a control vector bearing only the IRES-GFP cassette. Lentiviral vectors were produced by transient transfection of 293T cells as previously described (18).

**Cell lines and culturing conditions.** Human glioblastoma cell lines A172 and U87 (ATCC) were cultured as previously described (16). Mouse C17.2 NPCs, endogeneously expressing histologic marker protein  $\beta$ -galactosidase (19), were cultured in DMEM with 5% fetal bovine serum (Sigma), 2.5% horse serum (Sigma), 1 mmol/L sodium pyruvate (Cellgro), and 26 mmol/L sodium bicarbonate.

**Lentiviral transductions of glioma cells and NPCs.** U78 and A172 glioma cells were transduced with LV-Fluc-DsRed2 at a multiplicity of infection (MOI) of 2 in a growth medium containing 12  $\mu$ g/mL polybrene (Fisher Scientific), and 36 h later, cells were visualized for DsRed2 expression by fluorescence microscopy. Cells were passaged and Fluc expression was monitored at each passage by *in vitro* luciferase serial imaging as previously described (20). C17.2 NPCs were transduced with LV-S-TRAIL at a MOI of 5 in a growth medium containing 4  $\mu$ g/mL protamine sulfate and similarly visualized for green fluorescent protein (GFP) expression by fluorescence microscopy. S-TRAIL concentration in the conditioned culture medium was measured by ELISA with the TRAIL Immunoassay Kit (Biosource International) as previously described (17).

**Oligonucleotide transfection protocol.** The locked nucleic acid (LNA)-antimiR molecules were synthesized as unconjugated and fully phosphorothioated mixed LNA/DNA oligonucleotides with a 6-carboxyfluorescein

(FAM) moiety at the 5' end. The following sequences were synthesized: LNA-antimiR-21, 5'-FAM-tcagtctgataagcta-3', and LNA-control, 5'-FAM-cgtcagatgcgaatc-3' (kindly provided by Santaris Pharma). For transfection, oligonucleotides were allowed to form transfection complexes with LipofectAMINE 2000 reagent (Invitrogen), subsequently added to glioma cells, HEK293 cells, and primary mouse neuronal cultures at a final concentration of 50 nmol/L, and left to incubate for 8 h before medium change. To assess miR-21 inhibition in glioma cells, A172 and U87 cells were transfected with 1.5  $\mu$ g of pMIR-Report (firefly luciferase plasmid containing a perfect miR-21 binding site in the 3' untranslated region; Ambion) and 3  $\mu$ g of pRL-TK (*Renilla* luciferase plasmid; Promega) using LipofectAMINE 2000 as described above. After 24 h, firefly and *Renilla* luciferase activity were measured by quantitative luminescence assays (Dual Glo, Promega).

**Caspase-3/caspase-7 and cell viability assay.** U87 and A172 human glioma cells were plated at  $3 \times 10^3$  per well, transfected with LNAs, and assayed 48 h after transfection with five replicate wells per measurement. Cell viability and caspase activity *in vitro* were measured by quantitative luminescence assays. For viability, aggregate metabolic activity was measured using an ATP-dependent luminescent reagent (CellTiter-Glo, Promega). Caspase activity was determined with a caged, caspase-3/caspase-7-activatable DEVD-aminoluciferin (Caspase-Glo 3/7, Promega). Assays were done according to the manufacturer's instructions and plates were read in a luminometer at 1 s per plate. For *in vitro* S-TRAIL experiments, transfected glioma cells were incubated with 80 ng/mL S-TRAIL 24 h after transfection and left to incubate for another 24 h, after which caspase-3/caspase-7 activity and cell viability were determined as described above.

**Intracranial cell implantation.** Athymic nude mice (*nu/nu*, 6–7 weeks; Charles River Laboratories) were anesthetized as previously described (21). Three sets of experiments were done: (a) Fluc-DsRed2 expressing U87 cells were implanted at different concentrations (ranging from  $5 \times 10^4$  to  $3 \times 10^5$ ) in the right frontal lobe, and 24 h later, mice were imaged for Fluc activity as described below. (b)  $1 \times 10^5$  U87 glioma cells expressing Fluc-DsRed2 and transfected with anti-miR-21 or control LNA were trypsinized, harvested, and implanted stereotactically in the right frontal lobe [ $n = 3$  per group; from bregma, AP: -2 mm, ML: 2 mm V (from dura): 2 mm]. Mice were imaged for glioma burden by firefly luciferase (Fluc) activity as described in the following section. (c) U87-Fluc-DsRed2 cells ( $2 \times 10^5$ ) transfected with anti-miR-21-LNA or control LNA were mixed with either NPC-S-TRAIL or control transduced NPCs ( $1 \times 10^5$ ) in 5.5- $\mu$ L PBS and implanted stereotactically into the right frontal lobe of nude mice [ $n = 5$  per group; from bregma, AP: -2 mm, ML: 2 mm V (from dura): 2 mm] and mice were imaged as described below. All animal experiments were evaluated and approved by an institutional review board.

<sup>3</sup> Shah K, Hingtgen S, Kasmieh K, et al. Novel bimodal viral vectors and *in vivo* imaging reveal the fate of human neural stem cells in experimental glioma model. *J. Neuroscience* 2007, submitted for publication.

**In vivo bioluminescence imaging and tissue processing.** *In vivo* bioluminescence images were obtained using a cryogenically cooled high-efficiency charge-coupled device camera system (Roper Scientific). Mice were imaged for Fluc activity by injecting D-luciferin (4.5 mg/animal in 150- $\mu$ L saline) i.p. and recording photon counts 5 min after D-luciferin administration over 1 min. Post-processing and visualization were done as previously described (20). After glioma implantation on day 1, mice were imaged on days 2, 4, and 6. Immediately following the last imaging session, mice were sacrificed and brains were immersed in Tissue-Tek (Sakura Finetek) on dry ice and 7- $\mu$ m coronal brain sections were cut. DsRed2 fluorescence and LacZ staining for  $\beta$ -galactosidase, as previously described (17), were assessed by confocal microscopy (Bio-Rad).

**Statistical analysis.** Data were analyzed by Student's *t* test when comparing two groups and by ANOVA followed by Dunnett's post-test when comparing more than two groups. Data were expressed as mean  $\pm$  SE and differences were considered significant at  $P < 0.05$ .

## Results

The sequence-specific functional inhibition of miR-21 in glioma cells *in vitro* leads to increase in caspase levels followed by cell death (7). To test perseverance of this effect *in vivo*, we used U87 human glioma cells that express high levels of miR-21. Cells were stably transduced with LV-Fluc-DsRed2 (Fig. 1A), and a direct correlation between the number of cells and the emitted photons was shown *in vitro* (Fig. 1B) and *in vivo* (Fig. 1C) within the ranges tested. After transfection of Fluc-DsRed2-expressing U87 human glioblastoma cells, either with a FAM-labeled LNA/DNA gapmer oligonucleotide complementary to miR-21 (LNA-antimiR-21) or with a control LNA oligonucleotide (with a similar LNA/DNA gapmer design), oligonucleotides were shown to be present both in the cytoplasm and in the nucleus of the glioma cells (Fig. 2A), suggesting that the LNA-antimiR binds to the mature miR-21 as well as to pri-miR-21. In a parallel set of experiments, miR-21 inhibition in glioma cells was confirmed by a miR-21 luciferase sensor assay (Supplementary Fig. S1A). After validating miR-21 knockdown by LNA-antimiR-21, transfected Fluc-DsRed2 cells implanted intracranially into nude mice showed a sharp reduction in glioma

burden in the LNA-antimiR-21-transfected group starting after day 2 and leading to near eradication of miR-21 targeted tumors on day 6 (Fig. 2B and C), compared with undisturbed tumor proliferation in the LNA control-transfected groups ( $P = 0.0027$ ).

After confirming the *in vivo* applicability of miR-21-targeting monotherapy in gliomas, we hypothesized that miR-21 knockdown might additionally sensitize gliomas for locally delivered cytotoxic drugs through facilitation of apoptosis. For robust transduction, we used our recently engineered LV-S-TRAIL (18). NPCs were transduced with LV-S-TRAIL that harbors a cDNA encoding S-TRAIL as well as an IRES-GFP cassette, and transduction efficiency was confirmed by host cell GFP expression (Fig. 3A). Resulting NPC-S-TRAIL cells were viable and actively secreted S-TRAIL (220 ng/mL/ $10^6$  cells in generation-denaturation equilibrium; Fig. 3B), which resulted in the activation of caspase-3/caspase-7 and a considerable reduction in glioma cell viability in a dose-dependent manner in A172 (Fig. 3C) and U87 (Fig. 3D) glioma cells.

Next, to evaluate the synergistic effect of miR-21 knockdown and S-TRAIL *in vitro*, A172 and U87 glioblastoma cells were transfected with either control LNA (LNA-control) or LNA-antimiR-21 and subsequently incubated with NPC-S-TRAIL-derived S-TRAIL (80 ng/mL) for 24 h. At 48 h after transfection, cells were assayed for viability levels and caspase-3/caspase-7 activation. Both miR-21 knockdown and S-TRAIL treatment in isolation depressed viability (Fig. 4A and B) and caused caspase up-regulation (Fig. 4C and D) in both cell lines, implicating apoptosis to be involved as a cell death mechanism (22). However, marked additional caspase-associated cell killing was observed when treatments were combined ( $P < 0.005$ ; Fig. 3). Transfection of primary neuronal cultures and HEK293 cells with either control LNA or LNA-antimiR-21 did not affect their viability (Supplementary Fig. S1B and C). These findings indicate that, at least *in vitro*, knockdown of miR-21 before S-TRAIL administration sensitizes glioma cells for S-TRAIL cytotoxicity.

To determine if the presence of NPC-S-TRAIL influences the graft outcome of LNA-antimiR-21-treated glioma *in vivo*, we

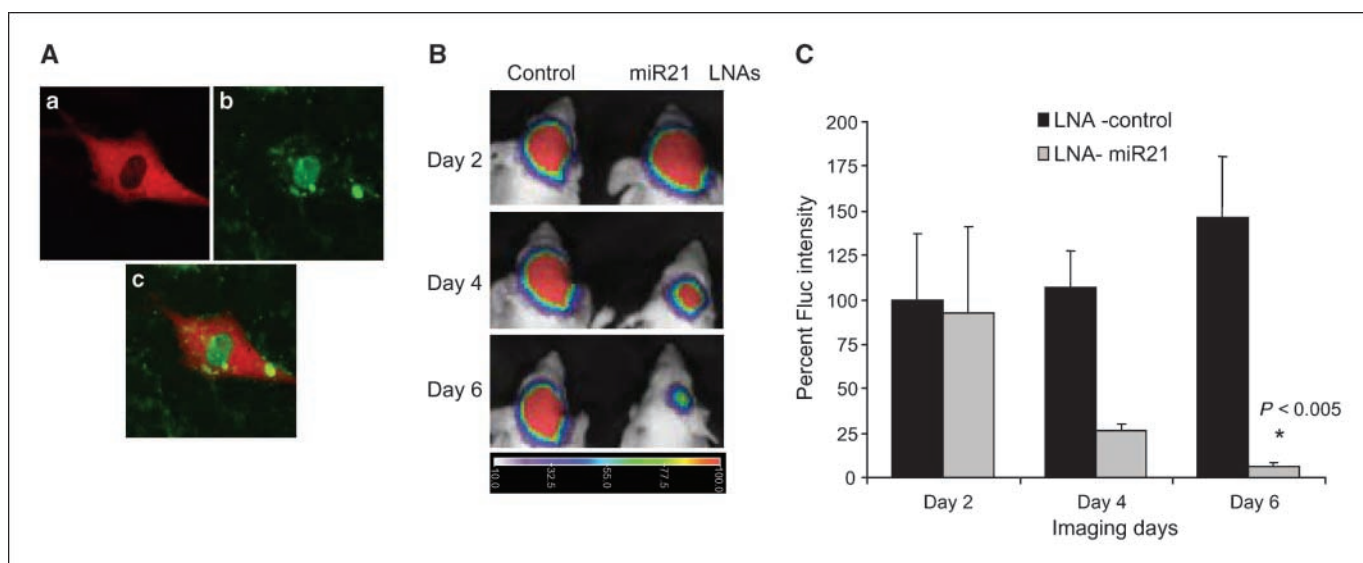
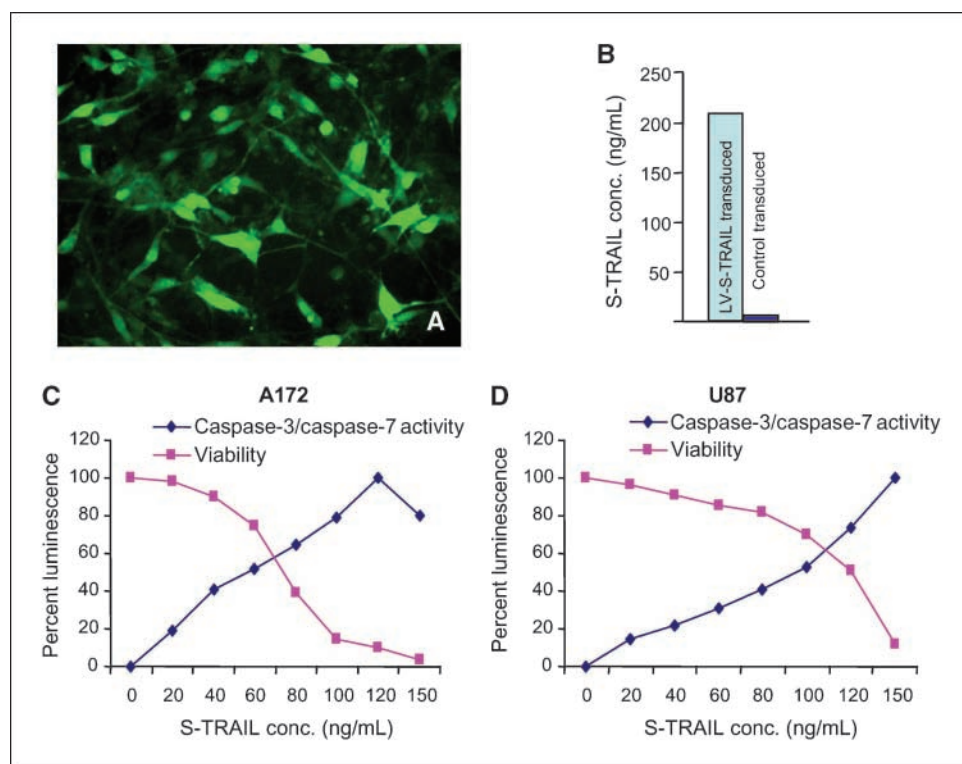


**Figure 2.** Knockdown of miR-21 in U87 glioma cells results in dramatic reduction of glioma growth *in vivo*. **A**, U87-Fluc-DsRed2 glioma cells transfected with FAM-labeled LNA-antimiR-21 or scrambled LNA control show cytoplasm and intranuclear or perinuclear localization (green). **B**, bioluminescent images revealing tumor growth of U87-Fluc-DsRed2 glioma cells transfected with either LNA-antimiR-21 or LNA control implanted stereotactically into the brains of nude mice. **C**, columns, quantified average relative bioluminescent intensities originating from tumors of LNA-miR-21 and LNA control groups on days 2, 4, and 6; bars, SE. Original magnification,  $\times 100$  (A, a-c).

**Figure 3.** NPCs lentivirally transduced to express S-TRAIL induce caspase-dependent cell death in glioma cells. **A**, NPCs transduced with LV-S-TRAIL, which also bears an IRES-GFP cassette. **B**, ELISA titering of S-TRAIL concentration in NPC-S-TRAIL and control-transduced NPC. **C** and **D**, cell viability and caspase-3/caspase-7 up-regulation of A172 (**C**) and U87 (**D**) glioma cells incubated with different concentrations of S-TRAIL. Original magnification,  $\times 20$  (**A**).



implanted a mix of LNA-antimiR-21-transfected Fluc-DsRed2 glioma cells and NPC-S-TRAIL or NPC-control ( $2 \times 10^5$  glioma cells and  $1 \times 10^5$  NPCs per injection) in the brain parenchyma and followed the glioma burden in real time by bioluminescence imaging (Fig. 5A). The number of glioma cells injected this time was twice the number used for evaluation of miR-21 therapy alone (Fig. 1) because we anticipated more intense tumor cell killing by incorporation of S-TRAIL in the therapeutic regimen. As in Fig. 1, we observed increasing glioblastoma size over time in the LNA control-transfected gliomas, whereas LNA-antimiR-21 treatment with NPC-control led to a considerable reduction in residual tumor volume (Fig. 5B). The presence of NPC-S-TRAIL in LNA control-pretreated gliomas already resulted in markedly decreased glioma burdens, superior even to miR-21 knockdown alone (Fig. 5B and C). Finally, the combination of miR-21 targeting and S-TRAIL-bearing NPCs caused a significant difference in the glioma volumes on day 4 compared with S-TRAIL monotherapy and completely eradicated tumors by day 6 of implantation ( $P < 0.02$ ; Fig. 5B and C). Histologic examination of brain sections revealed the presence of LacZ-expressing NPCs specifically in the DsRed2-positive gliomas and not in the surrounding normal brain tissue (Fig. 5D). These results reveal the robustness of the synergistic effect of miR-21 inhibition and S-TRAIL *in vivo*.

## Discussion

Recent evidence that miR-21 expression might be an important factor for tumorigenesis and apoptosis in specific cancers offers opportunities for improving glioma treatment strategies (3). In this study, we first evaluated intracranial graft survival of miR-21-antagonized gliomas, which showed a sharp reduction of tumor volumes *in vivo* compared with control-treated gliomas. Next,

we show that miR-21 suppression before S-TRAIL treatment, mediated by NPCs engineered to secrete S-TRAIL, leads to elevation of caspase activity and synergistic killing of glioma cells both *in vitro* and *in vivo*.

Previous studies by Chan et al. (7) showed that the introduction of complementary oligonucleotides into glioma cells with high miR-21 levels leads to reduction of glioma cell viability associated with an increase in activity of caspases (7). Here, we show that the effect of miR-21 knockdown *in vivo* leads to considerably decreased glioma volumes. However, the precise biological function of miR-21 remains elusive to this date. The increase in caspases escorting the decrease in viability on miR-21 knockdown would suggest an apoptosis-inhibiting effect, but it is unclear what factors mediate this effect. In a mouse model of breast carcinoma, Si et al. (23) recently showed knockdown of miR-21 to inhibit tumor cell growth *in vitro* and *in vivo* by effectuating an increase in apoptosis associated with down-regulation of Bcl-2 expression, a potent antiapoptotic regulatory factor (23). Because sequence analysis identified no direct targeting match between the miR-21-targeting antisense oligonucleotide and the Bcl-2 mRNA, direct binding of the antisense oligonucleotide to the Bcl-2 mRNA as a cause of this effect is highly unlikely. However, it is conceivable that miR-21 indirectly controls Bcl-2 expression through closely related apoptotic regulators. Intriguingly, whereas high miR-21 have been associated with enhanced proliferation in several tumors (6, 7, 23), one study has reported enhanced proliferation on miR-21 knockdown in noncancerous HeLa cells (24), which can only be rationalized by considering the complex nature of miRNA function. Namely, that one miRNA can have many ( $\sim 200$ ) mRNA targets, causing its effects to be dependent on locally available levels of biologically dominant substrates. Nevertheless, the consistent 5- to 100-fold up-regulation of miR-21 levels across primary and cultured glioma cell lines (7) and the marked



antitumor effect of miR-21 antagonism vindicate further exploration of therapeutic uses in parallel with more mechanistic research into miR-21 biology. A practical implication of the difficult nature of predicting miRNA function, however, is that early clinical studies of miRNA manipulation might reveal unforeseen side effects, particularly when miRNA-targeted therapies (either with oligonucleotides for down-regulation or with miRNA-encoding viral vectors for up-regulation) are not specifically homed to target sites.

The incorporation of the S-TRAIL gene into NPC is a useful way of circumventing its pharmacologic drawbacks such as delivery barriers (17). Our previous studies have shown that intracranially injected NPCs migrate from contralateral hemispheres to tumor burden and settle at the main tumor as well as microsatellite tumors (17). Furthermore, we have also shown that the intraventricular route is the most effective mode of NPC delivery (25), which minimizes travelling distance from implantation to target site. The latter is an important notion with regard to clinical application due to the larger travelling distances in the human brain. Importantly, migratory capabilities of NPCs are not affected by inserting the gene sequence for a secreted version of TRAIL, thereby creating biological "smart weapons," in which NPC-S-TRAIL display strong antitumor effects in murine gliomas *in vivo* (16, 17). Our results show that miR-21 antagonism and subsequent NPC-mediated S-TRAIL exert a marked synergistic caspase-associated cytotoxic effect in human glioblastoma cell lines *in vitro* and cause disruption of tumor growth *in vivo*. To our knowledge, these results are the first to describe the feasibility of

miRNA modulation for enhanced brain tumor therapy. Because the experimental model that we have used is artificial, a key issue for future development of miRNA therapeutics will be the adequate *in vivo* delivery of miRNA-antagonizing therapeutic agents. Recent evidence from breast cancer studies, however, indicates that inhibition of miR-21 levels by just more than 50% already leads to a significant decrease in tumor growth and an increase in caspase activity (23). Therefore, in the near future, direct introduction of preconstructed oligonucleotides might prove to be an effective approach. Thus far, two groups have reported significant suppression of specific miRNA levels across tissues following i.v., i.p., or s.c. administration of chemically modified oligonucleotides in experimental models (26, 27). Key to the success of these techniques seems to be the chemical modifications applied to the oligonucleotides to decrease vulnerability to exonucleases and endonucleases and to optimize bioavailability (28). LNA comprises a class of bicyclic conformational analogues of RNA that exhibit high Watson-Crick binding affinities to RNA and high stability in blood and tissues *in vivo* (29, 30). Previous studies along with the data presented here indicate that complementary, single-stranded LNA-antimiR oligonucleotides can mediate potent and specific inhibition of miRNA function *in vitro* (23, 31, 32). The improved miRNA recognition properties of LNA in Northern blot analyses and *in situ* hybridization (33–35), together with our data on miR-21 antagonism *in vivo*, imply that LNA-antimiR molecules may also be well suited as a novel class of potential therapeutics for disease-associated miRNAs. A practical problem in administering

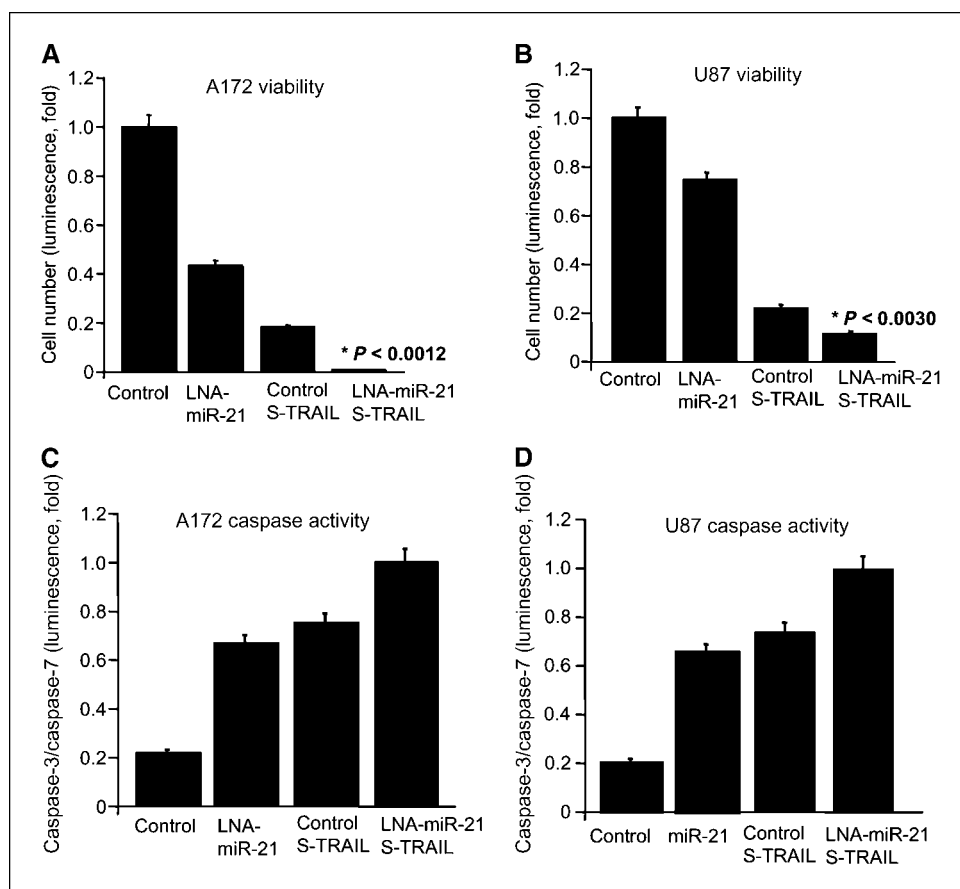


**Figure 4.** Knockdown of miR-21 in human glioblastoma cells leads to synergistic, caspase-associated cell killing in combination with NPC-derived S-TRAIL in culture. A172 and U87 human glioma cells were transfected with either LNA-antimiR-21 or LNA control (50 nmol/L), and 24 h later, cells were either treated with S-TRAIL (80 ng/mL) for or normal medium and assayed for viability and caspase activity at 48 h after transfection using ATP (and caspase)-dependent aminoluciferin assays. *A* and *B*, viability of A172 and U87 following miR-21 knockdown and incubation with S-TRAIL. *C* and *D*, associated levels of caspase activity following the same treatments.

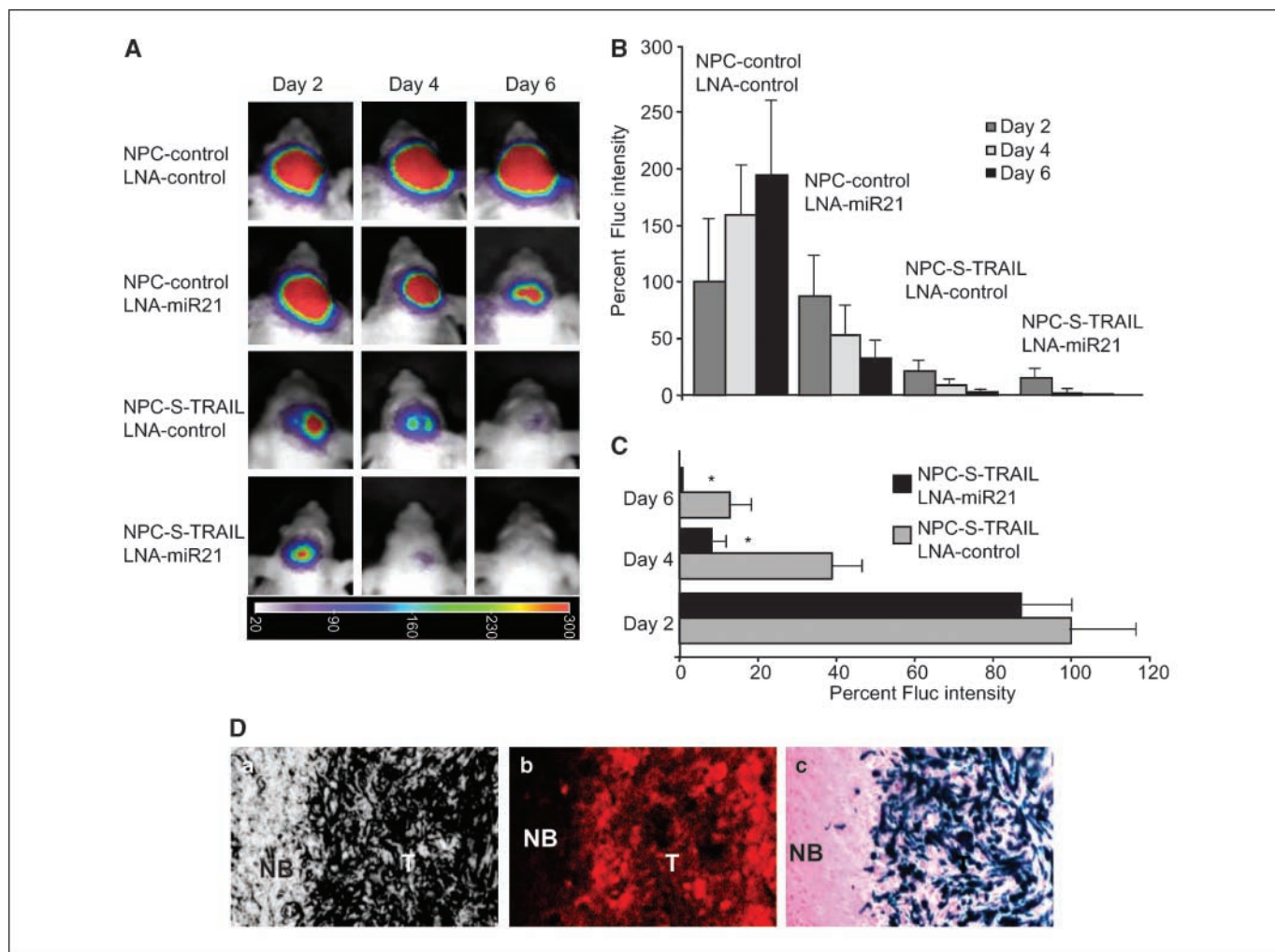


**Figure 5.** Knockdown of miR-21 and S-TRAIL display synergistic cell killing *in vivo*. **A**, *in vivo* bioluminescence imaging of tumor growth following intracranial implantation of U87-Fluc-DsRed2 glioma cells transfected with anti-miR-21 oligonucleotides (LNA-antimiR-21) or scrambled oligonucleotides (LNA control) and mixed with NPC either bearing S-TRAIL (NPC-S-TRAIL) or control transduced (NPC-control). Tumor expansion was serially imaged on days 2, 4, and 6. **B**, relative mean bioluminescent signal intensities after quantitation of *in vivo* images. **C**, columns, mean signal intensities extracted from **B** showing more clearly the differences in tumor growth following combined miR-21 and NPC-S-TRAIL therapy and solitary NPC-S-TRAIL therapy; bars, SE. **D**, immunohistochemical tracing of U87-Fluc-DsRed2 cells and NPCs by confocal microscopy. **a**, bright-light image; **b**, fluorescent image revealing DsRed2-expressing glioma cells; **c**, 5-bromo-4-chloro-3-indolyl- $\beta$ -D-galactopyranoside-stained tissue sections revealing presence of NPC. NB, normal brain; T, tumor.

oligonucleotides systemically is the effect on nontarget tissues. This could be remedied by oligonucleotide packaging (e.g., using lipid formulations) and conjugation with high-affinity molecules for guidance to target tissues using nanotechnology (36). Adjustments for facilitating crossing of the blood-brain barrier will also need attention. Although our LNA-miR-21 was not tested for blood-brain barrier crossing potential, previous data from other groups using similar formulations have revealed that *i.v.* administered oligonucleotides against other miRNAs can cause effective knockdown of miRNA levels in all tissues except the brain. It thus seems likely that targeting of LNA-miR-21 to the brain in the near future will require either intraventricular administration or packaging of oligonucleotides into lipophilic carrier constructs to facilitate blood-brain barrier passage. *In vivo* delivery of antisense oligonucleotides for miRNA knockdown will nonetheless require substantial additional research into both the miRNA biological function and the mechanisms of effective transport and homing.

In conclusion, we show that pretreatment of glioma cells with LNA-antimiR-21 molecules leads to synergistic antitumor efficacy both *in vitro* and *in vivo*. These results imply that selective miRNA antagonism might allow for sensitizing gliomas and other tumors for mainstay (or NPC-mediated S-TRAIL) therapy and could thus be of considerable interest for development of novel glioma therapies.

### Acknowledgments

Received 3/20/2007; revised 6/21/2007; accepted 7/3/2007.

**Grant support:** Stephen and Catherine Pappas Foundation (K. Shah); American Brain Tumor Association (K. Shah); NIH grants P50 CA86355 (R. Weissleder), P01 CA69246 (R. Weissleder), Brain Tumor Society grant, and NIH Exploratory/Developmental Research grant R21 CA116141 (A.M. Krichevsky).

The costs of publication of this article were defrayed in part by the payment of page charges. This article must therefore be hereby marked *advertisement* in accordance with 18 U.S.C. Section 1734 solely to indicate this fact.

We thank Joacim Elmén, Henrik Frydenlund, and Sakari Kauppinen from Santaris Pharma (Denmark) for providing miR-21 antisense DNA/LNA oligonucleotides, and Sakari Kauppinen and Joacim Elmén for helpful discussions.

## References

1. Bartel DP. MicroRNAs: genomics, biogenesis, mechanism, and function. *Cell* 2004;116:281–97.
2. Calin GA, Sevignani C, Dumitru CD, et al. Human microRNA genes are frequently located at fragile sites and genomic regions involved in cancers. *Proc Natl Acad Sci U S A* 2004;101:2999–3004.
3. Esquela-Kerscher A, Slack FJ. Oncomirs—microRNAs with a role in cancer. *Nat Rev Cancer* 2006;6:259–69.
4. Lu J, Getz G, Miska EA, et al. MicroRNA expression profiles classify human cancers. *Nature* 2005;435:834–8.
5. Calin GA, Liu CG, Sevignani C, et al. MicroRNA profiling reveals distinct signatures in B cell chronic lymphocytic leukemias. *Proc Natl Acad Sci U S A* 2004;101:11755–60.
6. Roldo C, Missiaglia E, Hagan JP, et al. MicroRNA expression abnormalities in pancreatic endocrine and acinar tumors are associated with distinctive pathologic features and clinical behavior. *J Clin Oncol* 2006;24:4677–84.
7. Chan JA, Krichevsky AM, Kosik KS. MicroRNA-21 is an antiapoptotic factor in human glioblastoma cells. *Cancer Res* 2005;65:6029–33.
8. Hanahan D, Weinberg RA. The hallmarks of cancer. *Cell* 2000;100:57–70.
9. Brown JM, Attardi LD. The role of apoptosis in cancer development and treatment response. *Nat Rev Cancer* 2005;5:231–7.
10. Visted T, Enger PO, Lund-Johansen M, Bjerkvig R. Mechanisms of tumor cell invasion and angiogenesis in the central nervous system. *Front Biosci* 2003;8:e289–304.
11. Simpson L, Galanis E. Recurrent glioblastoma multiforme: advances in treatment and promising drug candidates. *Expert Rev Anticancer Ther* 2006;6:1593–607.
12. Panner A, James CD, Berger MS, Pieper RO. mTOR controls FLIPS translation and TRAIL sensitivity in glioblastoma multiforme cells. *Mol Cell Biol* 2005;25:8809–23.
13. Rieger J, Naumann U, Glaser T, Ashkenazi A, Weller M. APO2 ligand: a novel lethal weapon against malignant glioma? *FEBS Lett* 1998;427:124–8.
14. Griffith TS, Anderson RD, Davidson BL, Williams RD, Ratliff TL. Adenoviral-mediated transfer of the TNF-related apoptosis-inducing ligand/Apo-2 ligand gene induces tumor cell apoptosis. *J Immunol* 2000;165:2886–94.
15. Kagawa S, He C, Gu J, et al. Antitumor activity and bystander effects of the tumor necrosis factor-related apoptosis-inducing ligand (TRAIL) gene. *Cancer Res* 2001;61:3330–8.
16. Shah K, Tung CH, Yang K, Weissleder R, Breakefield XO. Inducible release of TRAIL fusion proteins from a proapoptotic form for tumor therapy. *Cancer Res* 2004;64:3236–42.
17. Shah K, Bureau E, Kim DE, et al. Glioma therapy and real-time imaging of neural precursor cell migration and tumor regression. *Ann Neurol* 2005;57:34–41.
18. Kock N, Kasmieh R, Weissleder R, Shah K. Tumor therapy mediated by lentiviral expression of shBcl-2 and S-TRAIL. *Neoplasia* 2007;9:435–42.
19. Ryder EF, Snyder EY, Cepko CL. Establishment and characterization of multipotent neural cell lines using retrovirus vector-mediated oncogene transfer. *J Neurobiol* 1990;21:356–75.
20. Shah K, Tang Y, Breakefield X, Weissleder R. Real-time imaging of TRAIL-induced apoptosis of glioma tumors *in vivo*. *Oncogene* 2003;22:6865–72.
21. Shah K, Tung CH, Breakefield XO, Weissleder R. *In vivo* imaging of S-TRAIL-mediated tumor regression and apoptosis. *Mol Ther* 2005;11:926–31.
22. Hengartner MO. The biochemistry of apoptosis. *Nature* 2000;407:770–6.
23. Si ML, Zhu S, Wu H, Lu Z, Wu F, Mo YY. miR-21-mediated tumor growth. *Oncogene* 2007;19:2799–803.
24. Cheng AM, Byrom MW, Shelton J, Ford LP. Antisense inhibition of human miRNAs and indications for an involvement of miRNA in cell growth and apoptosis. *Nucleic Acids Res* 2005;33:1290–7.
25. Tang Y, Shah K, Messerli SM, Snyder E, Breakefield X, Weissleder R. *In vivo* tracking of neural progenitor cell migration to glioblastomas. *Hum Gene Ther* 2003;14:1247–54.
26. Krutzfeldt J, Rajewsky N, Braich R, et al. Silencing of microRNAs *in vivo* with “antagomirs.” *Nature* 2005;438:685–9.
27. Esau C, Davis S, Murray SF, et al. miR-122 regulation of lipid metabolism revealed by *in vivo* antisense targeting. *Cell Metab* 2006;3:87–98.
28. Krutzfeldt J, Poy MN, Stoffel M. Strategies to determine the biological function of microRNAs. *Nat Genet* 2006;38 Suppl:S14–9.
29. Koshkin AA, Singh SK, Nielsen P, et al. LNA (locked nucleic acids): Synthesis of the adenine, cytosine, guanine, 5-methylcytosine, thymine and uracil bicyclic nucleoside monomers, oligomerisation, and unprecedented nucleic acid recognition. *Tetrahedron* 1998;54:3607–30.
30. Fluiter K, ten Asbroek AL, de Wissel MB, et al. *In vivo* tumor growth inhibition and biodistribution studies of locked nucleic acid (LNA) antisense oligonucleotides. *Nucleic Acids Res* 2003;31:953–62.
31. Lecellier CH, Dunoyer P, Arar K, et al. A cellular microRNA mediates antiviral defense in human cells. *Science* 2005;308:557–60.
32. Orom UA, Kauppinen S, Lund AH. LNA-modified oligonucleotides mediate specific inhibition of microRNA function. *Gene* 2006;372:137–41.
33. Valoczi A, Hornyik C, Varga N, Burgyan J, Kauppinen S, Havelda Z. Sensitive and specific detection of microRNAs by Northern blot analysis using LNA-modified oligonucleotide probes. *Nucleic Acids Res* 2004;32:e175.
34. Wienholds E, Kloosterman WP, Miska E, et al. MicroRNA expression in zebrafish embryonic development. *Science* 2005;309:310–1.
35. Kloosterman WP, Wienholds E, de Bruijn E, Kauppinen S, Plasterk RH. *In situ* detection of miRNAs in animal embryos using LNA-modified oligonucleotide probes. *Nat Methods* 2006;3:27–9.
36. Toub N, Malvy C, Fattal E, Couvreur P. Innovative nanotechnologies for the delivery of oligonucleotides and siRNA. *Biomed Pharmacother* 2006;60:607–20.